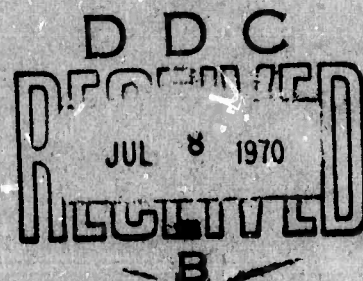# THE THREE-BODY RECOMBINATION AND DISSOCIATION OF DIATOMIC MOLECULES: A COMPARISON BETWEEN THEORY AND EXPERIMENT

Ven H. Shui, John P. Appleton and James C. Keck

April 1970

FLUID MECHANICS LABORATORY

DEPARTMENT OF MECHANICAL ENGINEERING

MASSACHUSETTS INSTITUTE OF TECHNOLOGY
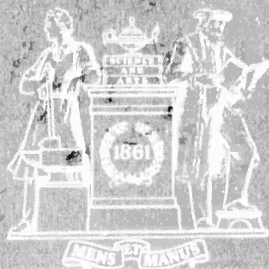
BLANK PAGE

THE THREE-BODY RECOMBINATION AND DISSOCIATION OF DIATOMIC MOLECULES:

A COMPARISON BETWEEN THEORY AND EXPERIMENT*

by

Ven H. Shui, John P. Appleton and James C. Keck

Fluid Mechanics Laboratory

Department of Mechanical Engineering
Massachusetts Institute of Technology

April 1970

SUMMARY

The modified phase-space theory of reaction rates has been used to predict the three-body recombination and dissociation rate coefficients of the diatomic gas molecules: H_2, N_2, O_2, F_2, Cl_2, Br_2, I_2, HF, HCl, CO and NO, in the presence of argon as a collision partner. The ability of the theory to quantitatively predict and correlate both low temperature recombination rate measurements and high temperature dissociation rate measurements is substantial. The success of the theory clearly illustrates the importance of the weak attractive forces between the recombining atoms and argon atoms for recombination at low temperatures, the marked reduction in the rates at high temperatures due to nonequilibrium distributions in the vibrational state populations of the molecules, and the major contributions to reaction progress via electronically excited molecular states at all temperatures for such molecules as N_2 and CO.

1.0 INTRODUCTION

In this paper we have used the modified phase-space theory of reaction rates, as developed by Keck and his co-workers[1-4] for three-body reactions, to predict the individual dissociation and recombination rate coefficients of a number of diatomic gases diluted in an argon heat bath.

We have adopted the phase-space theory approach because it represents the most general method of calculating the reaction rates of atomic and molecular systems whose interaction can be described by the motion of a representative point in the classical phase space of the reacting system. It can be shown that the more conventional classical reaction rate theories such as: unimolecular decay theory,[5] absolute reaction rate theory,[6] and available energy theory,[7] are all special cases of the phase-space theory. For a general discussion of these points we refer to Keck.[1]

Provided that the interaction potential of the three-body system can be defined, the modified phase-space theory which we have used here enables calculations to be made of dissociation and recombination rate coefficients which do not contain arbitary constants and undetermined "steric factors." Thus, when subsequent comparisons are made with reliable experimental measurements, it is usually possible to ascribe any significant disagreement between the theory and experiment to inadequacies in the assumed form of the basic three-body interaction potential. Such comparisons thus provide a method of making quantitative improvements to the interaction potentials.

BLANK PAGE

As we shall demonstrate by our comparisons, we have been able to obtain substantial quantitative agreement between theory and experiment and have thus correlated low temperature three-body recombination rate measurements (obtained for example, using the "discharge-flow-tube" technique) and high temperature "shock-tube" dissociation rate measurements for those cases where both types of data are available. The overall success of the theory clearly illustrates the importance of: 1) the attractive Van der Waal's forces between the recombining atoms and the argon atoms for recombination at low temperatures (such forces are, of course, invoked in the "relaxed complex" mechanism of recombination[8-11]), 2) the departure from an equilibrium distribution of the vibrational state populations[3,12] which, for either dissociation or recombination, occurs at an energy level on the order of kT below the dissociation limit, 3) the possible major contributions to the overall reaction rate due to reaction progress via electronically excited molecular states.[4]

The source experimental measurements which we have used in our comparisons were mainly suggested by recent review articles.[13-16] The particular cases which we have considered are the homonuclear diatomic gases: H_2, N_2, O_2, F_2, $C\ell_2$, Br_2, I_2, and the heteronuclear gases: HF, HCℓ, CO and NO.

In this paper we shall not include the detailed development of the modified phase-space theory since this can be found elsewhere.[1-4] A discussion of the theory and a complete summary of the working formulae has been given by Shui, Appleton and Keck[4] for the particular case of the dissociation and recombination of nitrogen in an argon heat bath.

We included in that paper a general account of the manner in which reaction progress via electronically excited states should be treated, together with a corrected version of the way in which departures from an equilibrium distribution in the vibrational state populations are allowed for. Thus, in Section 2.0 we shall give a brief summary of the working formulae and their physical interpretation, and devote the remainder of the paper to discussion of the comparisons between theory and experiment (Section 3.0), and our final conclusions (Section 4.0).

2.0 THEORETICAL CONSIDERATIONS

The type of reactions with which we are concerned are commonly written:

$$XY + M \underset{k_r}{\overset{k_d}{\rightleftharpoons}} X + Y + M \qquad (2.1)$$

and are observed to proceed in accordance with the overall rate equation:

$$d[XY]/dt = - k_d[XY][M] + k_r[X][Y][M]$$

$$= - d[X]/dt = -d[Y]/dt, \qquad (2.2)$$

where k_d and k_r are, respectively, the overall dissociation and recombination rate coefficients. For homonuclear diatomic molecules: X_2, Eq.(2.2) becomes:

$$d[X_2]/dt = - k_d[X_2][M] + k_r[X]^2[M]$$

$$= - d[X]/2dt . \qquad (2.3)$$

It is implied by the above rate equations that we restrict our attention to the calculation of reaction rates at times which are long by comparison with any "induction periods," i.e. the time intervals required to achieve close approximations to steady state distributions in the internal energy states of the molecules and atoms (see, for example, reference (17) for a discussion of the induction period due to vibrational relaxation). Therefore, both k_d and k_r are to be regarded as functions of temperature alone, and

their ratio equal to an equilibrium constant. If, as we shall assume
here,[4] each allowable electronic state of a particular species is
present in the reacting system in its local equilibrium proportion re-
lative to the total concentration of that species, then

$$k_d/k_r = \sum_p Q(p) \sum_q Q(q)/\sum_m Q(m)$$

$$= K_e(T) \tag{2.4}$$

where $Q(p)$ is the total particle partition function for atom X_p in
electronic state p, and $Q(q)$ and $Q(m)$ are similarly defined for atom
Y_q and molecule XY_m, respectively. The overall rate coefficients are
thus written in the forms:

$$k_d = \sum_m k_d(m|p,q) \; Q(m)/\sum_m \; Q(m) \tag{2.5}$$

and
$$k_r = \sum_m k_r(m|p,q) \; Q(p)Q(q)/\sum_p \; Q(p)\sum_q \; Q(q) \tag{2.6}$$

where $k_d(m|p,q)$ is the rate coefficient for dissociation of the molecule
in electronic state m, to atoms in electronic states p and q, and $k_r(m|p,q)$
is the corresponding recombination rate coefficient. We note that as a
consequence of the Born-Oppenheimer separation, the specification of a
particular molecular state automatically identifies the atomic states to
which the molecule dissociates.

For most diatomic molecules and their atoms it is usually true
that the ground state partition functions, e.g. $Q(p=0)$, are much greater
than the partition functions of the first and higher excited states for

temperature ranges of normal interest, and thus, the overall rate coefficients may be approximately rewritten in the forms:

$$k_d = \sum_m k_d(m|0,0)Q(m)/Q(m=0) \qquad (2.7)$$

and

$$k_r = \sum_m k_r(m|0,0), \qquad (2.8)$$

so that,

$$k_d/k_r = Q(p=0)Q(q=0)/Q(m=0) \qquad (2.9)$$

is the equilibrium constant based on ground state concentrations only. One important exception for which the above approximate equations are not valid over the whole temperature range of our interest is the case of oxygen. The ^3P "ground" state oxygen atom actually consists of three states $^3P_2$, $^3P_1$, and $^3P_0$, with slightly different energy levels: 0, 229°K, and 326°K, and with corresponding degeneracies of 5, 3, and 1, respectively. Thus, at temperatures below about 1000°K, the exact equations (2.5) and (2.6) have been used here.

The modified phase-space theory enables us to calculate the individual recombination (or dissociation) rate coefficients: $k_r(m|p,q)$, in terms of what Keck[1] has called the "barrier rate" coefficient: $k_r^B(m|p,q)$. This latter quantity, which represents a rigorous upper bound to the actual rate coefficient, requires modification by a statistical correction factor: (N/N_0), and nonequilibrium correction factors: (k/k_e), to obtain $k_r(m|p,q)$.

The barrier rate is given in terms of the total one-way flow of points, representative of the three-body complex (X-Y-M), in the classical

phase space across a suitably defined surface which separates the
initial states of the system - the reactants, from their final states -
the products. The phase space surface which most logically separates
molecules from atoms is the "barrier surface" which is defined by the
constraints

$$E_{XY} - B_{XY} = 0 \; ; \; E > 0 \tag{2.11}$$

where E is the total internal energy of the three-body system (X-Y-M),
E_{XY} is the internal energy of the recombining atoms (X-Y), and B_{XY} is
the height of the rotational energy barrier. For recombination, the
product state is defined by $(E_{XY} - B_{XY}) < 0$, and the reactants by
$(E_{XY} - B_{XY}) > 0$. By following this prescription, Keck[1,2] has derived
the following expression for the barrier rate coefficient:

$$k_r^B(m|p,q) = 4\pi^2 \, fa^2 z_2^2 (z_2 - z_1)(8kT/\pi\mu_{XY})^{1/2}[1 - \exp(- B_m/kT)] \tag{2.12}$$

where $f = g_{XY_m}/g_{X_p} g_{Y_q}$, is the electronic degeneracy factor, μ_{XY} is the
reduced mass of the molecule XY, and B_m is the maximum height of the
rotational barrier.

For the purpose of providing a simple physical explanation for
the form of Eq. (2.12), we may point out that the factor: $4\pi z_2^2(z_2 - z_1)$,
is a molecular volume proportional to the number of atom pairs (X-Y),
close enough to recombine; whereas, the factor: $\pi a^2(8kT/\pi\mu_{XY})^{1/2}$, is a
rate constant proportional to the frequency at which the (X-Y) pairs are
stabilized under the influence of the third body M. The reason for the

appearance of the reduced mass μ_{XY}, for the recombining atoms in the velocity term rather than the reduced mass $\mu_{XY,M}$ for collisions of (X-Y) with M, is that in the "barrier rate" it is the rate of momentum transfer from M to (X-Y), rather than the collision rate of M with (X-Y), which controls the recombination. The additional factor: $[1 - \exp(- B_m/kT)]$, simply eliminates those atom pairs which cannot form bound molecules because of their excessive orbital angular momentum.

The characteristic lengths a, z_1, and z_2 are all temperature dependent and may be determined in terms of the characteristic potential parameters which are used to describe the interaction potential of the three-body system (X-Y-M). We have assumed that the interaction potential is given as the sum of two potentials:

$$V_0 = V_{XY} + V_{1M} \tag{2.13}$$

where V_{XY} is the potential of the recombining atoms (X-Y), and V_{1M} is the potential between one of the atoms and the third body M; $V_{1M} \equiv V_{XM}$, when the internuclear distance r_{XM} is smaller than r_{YM}, and $V_{1M} \equiv V_{YM}$, when $r_{XM} > r_{YM}$. Keck has termed this the "dumb-bell" model of the interaction potential. In our calculations we have used the Morse potential function:

$$V(r) = U\{[1 - \exp(- \beta(r - r_e))]^2 - 1\} \tag{2.14}$$

to represent both V_{XY} and V_{1M}, with appropriate suffices added to the potential parameters U, β, and r_e to identify the particular two-body

potential under consideration. Graphical solutions for a, z_1, and z_2 as functions of the appropriate potential parameters have been given elsewhere.[4] However, we should point out that the phase-space theory, in the form which we have used, tacitly assumes that all species, including the complexes: X.M and Y.M, are present in their local equilibrium proportions, and as a consequence, the major temperature dependence of the effective collision cross-section (πa^2), is determined by a factor: $\exp(U_{1M}/kT)$.

Unfortunately, the barrier surface which is chosen to separate reactants from products in the phase space is not unique in the sense that representative point trajectories may cross and re-cross it several times. Since k_r^B is calculated on the basis of the total one-way crossing rate, it does represent an upper bound to the actual rate.

Keck[18] has investigated this effect using Monte Carlo methods which sample phase-space trajectories which cross the "barrier" surface, and by integration of the classical equations of motion in both time-wise directions, has obtained a statistical determination of the fraction (N/N_0), in which N is the number trajectories which result in a complete one-way reaction, and N_0 is the total number of trajectories sampled. Thus, we regard (N/N_0) as a statistical correction factor which multiplies the value of k_r^B given by Eq. (2.12). Numerical values for (N/N_0) can be found in reference (18) and semi-empirical formulae in references (1) and (4).

The nonequilibrium correction factor which we have used here is based on the results of the investigation by Keck and Carrier[3] of the coupled vibration-dissociation-recombination process for a dilute mixture

of diatomic molecules in a heat bath of inert collision partners.
After the initial vibrational relaxation transient, it was found that
for dissociation, the steady-state vibrational level population is very
nearly Boltzmann except near the dissociation limit (within a few kT of
the dissociation limit) where the levels are underpopulated; for recombi-
nation, the steady-state distribution is Boltzmann near the dissociation
limit, but the lower levels are underpopulated. Because of this, the
steady-state rate coefficients: k_d and k_r, are smaller than the equi-
librium rate coefficients: k_{de} and k_{re}, although their ratio is very
nearly equal to the equilibrium constant; i.e.,

$$k_d/k_r = k_{de}/k_{re} = K_e(T) \tag{2.15}$$

By assuming a classical Morse oscillator to represent the molecule and
an exponential form to represent the repulsive interaction between the
collision partner and the molecule, Keck and Carrier solved the appropri-
ate master equation to give a closed form expression for the nonequilib-
rium correction factors: (k/k_e).

In reference (4) it was pointed out that when an attractive minimum
exists in the two-body potentials V_{iM}, there are four contributions to the
barrier rate coefficient, viz.

$$k_r^B(m|p,q) = k_{rX+}^B + k_{rX-}^B + k_{rY+}^B + k_{rY-}^B \tag{2.16}$$

corresponding to four distinctly different configurations of the three-
body complex for which the momentum transfer rate between (X-Y) and M

are maximum. It is therefore necessary to evaluate a nonequilibrium correction factor, i.e. $(k/k_e)_{i\pm}$, for each of these configurations, thereby obtaining an expression for the actual rate coefficient in the form:

$$k_r(m|p,q) = \left[k^B_{rX+}(k/k_e)_{X+} + k^B_{rX-}(k/k_e)_{X-} \right.$$

$$\left. + k^B_{rY+}(k/k_e)_{Y+} + k^B_{rY-}(k/k_e)_{Y-} \right] (N/N_0) \qquad (2.17)$$

3.0 COMPARISONS BETWEEN THEORY AND EXPERIMENT

The potential parameters r_{eiM}, for the Morse potential which describe the interactions between the separated atoms X and Y, and the collision partner M, were first estimated from empirical rules, suggested by Bernstein and Muckerman,[19] which related r_e to the radii of the principal maxima in the radial distribution functions of the ground state atoms.[20] The potential energy well depths: U_{iM}, were first estimated by applying the Badger-Johnston relation[19] in the manner suggested by Bernstein and Muckerman. The remaining Morse potential parameters, β_{iM}, were obtained by setting $2\beta_{iM} = 1/L_{iM}$, where L_{iM} is the range of an effective exponential potential, given by the Mason-Vanderslice extrapolation formula.[21] These estimates of r_{eiM}, U_{iM} and β_{iM} are summarized in Table I.

The spectroscopic data for the molecules which are required in the calculations are summarized in Table II. These data were mostly taken from Herzberg,[22] Gilmore,[23] Krupenie,[24] and the JANAF Tables.[25]

The source references for the experimental data have, to a large extent, been taken from the review articles cited previously, although, we have attempted to include in our comparisons some more recent investigations. Because of space limitations, we clearly cannot present a critical review of the many experimental investigations.

For those molecules where both low temperature recombination rate data and high temperature dissociation rate data are available, we have made the comparisons on the basis of the inferred recombination rate coefficients. For those molecules where only dissociation rate data are

available, we have made the comparisons using the usual Arrhenius plots.
Only for the case of oxygen have both methods of comparison been used.
We again stress that the theoretical predictions were made on the assump-
tion that argon was the collision partner which, in the majority of the
experimental investigations chosen for comparison, was the case.

3.1 Hydrogen

Figure 1 shows our prediction of $k_r(X \ ^1\Sigma_g^+|^2S, ^2S)$, given by the
lower dashed line, as compared with the direct recombination rate measure-
ments[26,27] and the recombination rate coefficients inferred from the
high temperature dissociation rate measurements for hydrogen.[28-31]
The disagreement between our prediction and the highest high temperature
measurements by Hurle, Jones, and Rosenfeld[28] is about a factor of two.
However, our agreement with the experiment results of Sutton,[30] and
Myerson and Watt[31] and the low temperature recombination measurements
of Larkin and Thrush[26,27] is excellent. Thus, in view of the possible
experimental scatter, as indicated by the cross-hatched area which corres-
ponds to the error estimate given in reference (28), we conclude that our
prediction is good.

The upper dashed line in Fig. 1 shows our prediction of the equi-
librium rate coefficient: $k_r^B(X \ ^1\Sigma_g^+|^2S, ^2S)(N/N_0)$. By comparing this with
the actual rate we see that the correction due to the nonequilibrium distri-
bution in the vibrational state populations is significant over the entire
temperature range of the experiments, but becomes most pronounced at high
temperatures. The magnitude of the nonequilibrium correction was found
to be similar for all of the homonuclear molecules considered, although

any given set of low and high temperature data. Our preference for only changing U_{NAr}, resulted from our observation[4] that the high temperature prediction of k_d thus obtained agreed remarkably well with the measurements due to Appleton, Steinberg and Liquornik,[36] and because there is recent independent evidence from molecular beam scattering experiments due to Jordan, Colgate, Amdur and Mason,[37] which supports the value of β_{NAr} given by the Mason Vanderslice extrapolation formula.[21]

3.3 Oxygen

Figure 3 shows our prediction of $k_r(X\ ^3\Sigma_g^- | ^3P, ^3P)$, lower dashed curve, and our prediction of the sum of the individual recombination rate coefficients corresponding to all the electronic states of oxygen listed in Table II, upper dashed curve.

Improved agreement with the temperature dependence of the low temperature measurements due to Campbell and Thrush[32] could be obtained by increasing our estimate of U_{OAr}. However, this would also entail a reduction in our estimate of r_{eOAr} and a change in β_{OAr} for the theoretical value of k_r to still pass through the main body of the high temperature data. We have not pursued this curve fitting procedure in the case of oxygen since we have rather arbitarily assumed that each combination of the $^3P_{2,1,0}$ states of the oxygen atoms interact without restriction along each of the potential energy curves of the molecule listed in Table II. We have thus violated the "non-crossing" rule of potential energy surfaces which may result in significant errors in our calculation of k_r at the low temperatures where the energy spacing between the ^3P states are comparable with kT.

It is interesting to note that the recombination rates inferred from the dissociation rate measurements due to Watt and Myerson[40] agree quite well with the prediction of $k_r(^3\Sigma_g^-|^3P,^3P)$, lower dashed curve. This is indeed precisely what might be expected, since Watt and Myerson used the technique of atomic line resonance absorption to monitor the production of oxygen atoms behind shock waves. Due to the high sensitivity of the technique, they were only able to measure the initial rate of dissociation over a period which, although encompassing the ground state vibrational relaxation transient, quite possibly did not extend into the region where the higher electronic states assumed their local equilibrium concentrations.

Figure 4 shows an Arrhenius plot of the various dissociation rate measurements[40-43] together with our theoretical prediction of k_d. It is apparent that the theory underestimates some of Wray's[41] measurements and Camac and Vaughan's[42] measurements by about a factor of two to three. However, it should be pointed out that within the temperature range where the measurements overlap, there is disagreement between them of at least a factor of two.

3.4 Fluorine, Chlorine, Bromine, and Iodine

An Arrhenius plot of the dissociation rate measurements for fluorine due to Johnson and Britton[44] is shown in Figure 4 together with our prediction of $k_d(X\ ^1\Sigma_g^+|^2P,^2P)$. Although there is a relatively large scatter amongst the experimental data, the theoretical prediction does pass through the main body of the data and thus appears to be satisfactory.

The comparisons between the a priori theoretical predictions of the recombination rate coefficients (i.e. theoretical predictions obtained

using potential parameters derived from empirical rules - dashed lines in Figs. 6-8) and the experimental measurements for Cl_2, Br_2, I_2, illustrate a definite trend. For the case of chlorine, Fig. 6, the theoretical prediction lies below the experimental data over the major portion of the temperature range and has a less steep temperature dependence than that indicated by the combined measurements. On the other hand, Fig. 8 for iodine shows that the a priori prediction of $[k_r(X \, {}^1\Sigma_g^+ | {}^2P_{3/2}, {}^2P_{3/2}) + k_r(A \, {}^3\Pi_{1u} | {}^2P_{3/2}, {}^2P_{3/2})]$ is greater than the measurements by about a factor of two, but exhibits a temperature dependence which is in reasonable agreement with the combined measurements. The comparison for the case of bromine, Fig. 7, appears to be an intermediate situation, i.e. the prediction of the recombination rate is greater than the bulk of the experimental data at temperatures above $300^\circ K$, but at lower temperatures it lies below an extrapolation of the experimental results.

Having recognised these trends and again in view of our previous comment that the major temperature dependence of k_r is largely determined by the factor: $\exp(U_{iM}/kT)$, at low temperatures, whereas, it is roughly proportional to r_{eiM}^2, independently of temperature, we adjusted the values of U_{iM} and r_{eiM} ($i = Cl$, Br, I) as shown in Table I, to obtain the full theoretical curves illustrated in Figs. 6-8. It is apparent that this fitting procedure has enabled us to correlate a large fraction of the experimental data for dissociation and recombination of the halogens, and as a consequence, we suggest that the derived potential parameters, particularly U_{ClAr} and U_{BrAr}, are more realistic than those given by the empirical rules.

The above curve fitting procedure follows in much the same spirit as Porter[10] chose to view the binding energy of the relaxed complex: I.M, as an adjustable parameter for correlating iodine recombination measurements, and more recently, as Ip and Burns[11] similarly chose to view the binding energy of the relaxed complex: Br.M, as an adjustable parameter for correlating their bromine recombination measurements. For the I.Ar complex, Porter suggested: $U_{I.Ar} \simeq 500^{\circ}K$, and for Br.Ar, Ip and Burns suggested: $U_{Br.Ar} \simeq 450^{\circ}K$, c.f. Table I.

3.5 Hydrogen Fluoride and Hydrogen Chloride

The Arrhenius plots of the dissociation rates of hydrogen fluoride and hydrogen chloride, illustrated in Figures 9 and 10, show that our predictions of the dissociation rate coefficients are much too low by comparison with the experimental measurements.[61-65] We have, however, also plotted the barrier rate coefficients: $k_d^B(X {}^1\Sigma^+|{}^2S,{}^2P)$, which, although they are too large (as we should expect), nevertheless, have about the right temperature dependence. We believe that the reason why our predictions of the rate coefficients underestimate the measured rates is that our estimate of the statistical correction factors: $(N/N_0) \lesssim 0.01$, and the nonequilibrium correction factors: $(k/k_e) \simeq 0.01$, are too small. The correlation formulae which we have used[3,4,17] to estimate the values of (N/N_0) and (k/k_e) were deduced using the results of Monte Carlo trajectory calculations and master equation solutions in which the recombining molecules and the collision partners had similar masses. We believe that the mechanics of reacting collision processes in which one of the recombining atoms has a very small mass is sufficiently different from those

cases considered in reference (18), that the correlation formula is no longer valid. Further work on this problem is in progress.

3.6 Carbon Monoxide and Nitric Oxide

Figure 11 shows an Arrhenius plot of the measured dissociation rate coefficients[66-69] of carbon monoxide together with our predictions of $k_d(X\ {}^1\Sigma_g^+|{}^3P,{}^3P)$, lower dashed curve, and $\sum_m k(m|{}^3P,{}^3P)$, upper dashed curve (see Table II for identification of the electronic states included). The prediction which includes all of the excited state contributions is nearly an order of magnitude greater than $k_d(X\ {}^1\Sigma_g^+|{}^3P,{}^3P)$ and, consequently, is in better agreement with the measurements. Small increases in either r_{e1M} or β_{1M} could be made which would allow the theoretical value of $\sum_m k_d(m|{}^3P,{}^3P)$ to correlate quite well with the bulk of the experimental data. The fact that $\sum_m k_d(m|{}^3P,{}^3P)$ does agree so well with the experimental measurements is quite gratifying since Fairbairn[68] and Appleton, Steinberg, and Liquornik[69] (point values in Fig. 11) did observe an induction time immediately following the shock wave, prior to the onset of a steady-state dissociation, which they attributed to the time required to populate excited molecular states.

Figure 12 shows our predictions of $k_r(X\ {}^2\Pi|{}^4S,{}^3P)$, lower dashed curve, and $[k_r(X\ {}^2\Pi|{}^4S,{}^3P) + k_r(a\ {}^4\Pi|{}^4S,{}^3P)]$, upper dashed curve, together with the few experimental rate measurements for nitric oxide which are available.[38,70] The agreement is fairly good, although, it would certainly be desirable to have more extensive measurements of the rates of this important molecule. Again, as in the case of CO, a slight increase in the value of β_{1Ar} would raise the high temperature rate coefficients and place the theoretical predictions in closer agreement with Wray's dissociation rate measurements.[70]

4.0 CONCLUSIONS

In the foregoing, we have demonstrated that modified phase-space trajectory calculations of the reaction rate coefficients of diatomic molecules in an argon heat bath are able to correlate both the very high and low temperature rate measurements. The exceptions to this conclusion appear to be those diatomic molecules which have disparate atomic masses such as HF and HCℓ.

Apart from the recognition that reaction progress via excited molecular states is likely to be important in certain cases, e.g. N_2 and CO, the quantitative success of the theory is clearly dependent on prior knowledge of the interaction potential between the recombining atom pairs and the collision partner. However, on the basis of the comparisons presented here, we suggest that valid quantitative information on the interatomic potentials can be obtained from a proper synthesis of the phase-space theory and reliable experimental data obtained over a wide temperature range. Such a view is, of course, entirely in keeping with existing methods which have been widely used for deducing inter-molecular potential information at thermal energies from measurements of transport properties.

Finally, we should point out that for those cases where the collision partners are highly reactive, e.g.

$$X + X + X \rightleftharpoons X_2 + X,$$
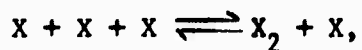
the "dumb-bell" model for the three-body interaction potential and the approximations used in deriving the expression for k_r^B are no longer

valid. A more realistic model for the interaction potential must be
assumed and a more detailed analysis will be involved in the calculation.
Work in this direction is being persued at this laboratory on the
(H + H + H) system which, hopefully, will shed some light on the question
as to why, in dissociation and recombination processes, the parent atoms
are much more efficient third-body collision partners than those which
are "inert".

REFERENCES

1. Keck, J. C., Adv. Chem. Phys. 13, 85 (1967).

2. Keck, J. C., J. Chem. Phys. 32, 1035 (1960).

3. Keck, J. C. and Carrier, G. F., J. Chem. Phys. 43, 2284 (1965).

4. Shui, V. H., Appleton, J. P., and Keck, J. C.,submitted to J. Chem.
    Phys. (A preliminary report version of this paper appeared as:
    "The Dissociation and recombination of Nitrogen: A Comparison
    Between Theory and Experiment," Fluid Mechanics Lab Report 70-2,
    Dept. of Mechanical Engineering, M. I. T., February, 1970).

5. Slater, N. B., Theroy of Unimolecular Reactions, Cornell University
    Press, 1959.

6. Glasstone, S., Laidler, K., and Eyring, H., The Theory of Rate
    Processes, McGraw-Hill Book Company, 1941.

7. Fowler, R. H. and Guggenheim, E. A., Statistical Thermodynamics,
    The Cambridge University Press, 1952.

8. Rice, O. K., J. Chem. Phys. 9, 258 (1941).

9. Bunker, D. L. and Davidson, N., J. Am. Chem. Soc., 80, 5085 (1958).

10. Porter, G., Disc. Faraday Soc. 33, 198 (1962).

11. Ip, J. K. K. and Burns, G., J. Chem. Phys. 51, 3414 (1969).

12. Osipov, A. I. and Stupochenko, E. V., Sov. Phys. Usp. 6, 47 (1963).

13. Kaufman, F., Ann. Rev. Phys. Chem. 20, 45 (1969).

14. Belford, R. L. and Strehlow, R. A., Ann. Rev. Phys. Chem. 20,
    247 (1969).

15. Schofield, K., Planetary Space Sci. 15, 643 (1967).

16. Johnston, H. S., "Gas Phase Reaction Kinetics of Neutral Oxygen
    Species," NSRDS-NBS 20 (1968).

17.   Brau, C. A., Keck, J. C., and Carrier, G. F., Phys. Fluids 9, 1885 (1966).

18.   Keck, J. C., Disc. Faraday Soc. 33, 173 (1962).

19.   Bernstein, R. B. and Muckerman, J. T., Adv. Chem. Phys. 12, 389 (1967).

20.   Waber, J. T. and Cromer, Don T., J. Chem. Phys. 42, 4116 (1965).

21.   Mason, E. A. and Vanderslice, J. T., J. Chem. Phys. 28, 432 (1958).

22.   Herzberg, G., Spectra of Diatomic Molecules, D. Van Nostrand Co., Inc., New York, (1950).

23.   Gilmore, F. R., "Basic Energy-Level and Equilibrium Data for Atmospheric Atoms and Molecules," Memorandum RM-5201-ARPA (March 1967), The Rand Corporation, Santa Monica, California.

24.   Krupenie, P. H., "The Band Spectrum of Carbon Monoxide,"(National Standard Reference Data Series), National Bureau of Standards - 5, (1966).

25.   JANAF Thermochemical Tables, Prepared under the auspices of the Joint Army-Navy-Air Force Thermochemical Panel at the Thermal Research Laboratory, The Dow Chemical Co., Midland, Michigan, 1961.

26.   Larkin, F. S. and Thrush, B. A., Tenth Symposium (International) on Combustion, p. 397, The Combustion Institute (1965).

27.   Larkin, F. S., Can. J. Chem. 46, 1005 (1968).

28.   Hurle, I. R., Jones, A., and Rosenfeld, J. L. J., Proc. Roy. Soc. A 310, 253 (1969).

29.   Jacobs, T. A., Giedt, R. R., and Cohen, N., J. Chem. Phys. 47, 54 (1967).

30.   Sutton, E. A., J. Chem. Phys. 36, 2923 (1962).

31.   Myerson, A. L. and Watt, W. S., J. Chem. Phys. 49, 425 (1968).

32.   Campbell, I. M. and Thrush, B. A., Proc. Roy. Soc. A 296, 201 (1967).

33.   Clyne, M. A. A. and Stedman, D. H., J. Phys. Chem. 71 3071 (1967).

34.   Byron, S., J. Chem. Phys. 44 1378 (1966).

35.   Cary, B., Phys. Fluids 8 26 (1965).

       Wray, K. L. and Byron, S., ibid 9, 1046 (1966).

       Cary, B., ibid 9, 1047 (1966).

36.   Appleton, J. P., Steinberg, M., and Liquornik, D. J., J. Chem.
       Phys. 48, 599 (1968).

37.   Jordan, J. E., Colgate, S. O., Amdur, I., and Mason, E. A., J. Chem.
       Phys. 52, 1143 (1970).

38.   Campbell, I. M. and Thrush, B. A., Proc. Roy. Soc. A 296, 222 (1967).

39.   Wray, K. L., J. Chem. Phys. 38, 1518 (1963).

40.   Watt, W. S. and Myerson, A. L., "Atom Formation Rates Behind Shock
       Waves in Oxygen," Cornell Aeronautical Laboratory, Inc., CAL AD-1689-A9,
       February, 1969.

41.   Wray, K. L., Tenth Symposium (International) on Combustion, p. 523,
       The Combustion Institute (1965).

42.   Camac, M. and Vaughan, A., J. Chem. Phys. 34, 460 (1961).

43.   Anderson, O. L., "Shock-Tube Measurement of Oxygen Dissociation
       Rates in Argon," United Aircraft Corporation Research Labs, Report
       R-1828-1 (1961).

44.   Johnson, C. D. and Britton, D., J. Phys. Chem. 68, 3032 (1964).

45.   Clyne, M. A. A. and Stedman, D. H., Trans. Faraday Soc. 64, 2698 (1968).

46. Diesen, R. W. and Felmlee, R. W., J. Chem. Phys. 39, 2115 (1963).

47. Van Thiel, M., Seery, D. J. and Britton, D., J. Phys. Chem. 69, 834 (1965).

48. Carabetta, R. A. and Palmer, H. B., J. Chem. Phys. 46, 1333 (1967). Erratum: ibid 47, 2202 (1967).

49. Jacobs, T. A. and Giedt, R. R., J. Chem. Phys. 39, 749 (1963).

50. Ip, J. K. K. and Burns, G., Disc. Faraday Soc. 44, 241, 278 (1967).

51. Ip, J. K. K. and Burns, G., J. Chem. Phys. 51, 3425 (1969).

52. Boyd, R. K., Burns, G., Lawrence, T.R. and Lippiatt, J. H., J. Chem. Phys. 49, 3804 (1968).

53. Johnson, C. D. and Britton, D., J. Chem. Phys. 38, 1455 (1963).

54. Warshay, M., NASA TN D-3502 (Washington, D. C., July, 1966). NASA TN D-4795 (Washington, D. C., Sept. 1968).

55. Britton, D., J. Phys. Chem. 64, 742 (1960).

56. Palmer, H. B. and Hornig, D. F., J. Chem. Phys. 26, 98 (1957).

57. Bunker, D. L. and Davidson, N., J. Am. Chem. Soc. 80, 5085, 5090 (1958).

58. Porter, G. and Smith, J. A., Proc. Roy. Soc. A 261, 28 (1961).

59. Britton, D., Davidson, N., Gehman, W., and Schott, G., J. Chem. Phys. 25, 804 (1956).

60. Troe, J. and Wagner, H. G., Z. Physik. Chem. 55, 326 (1967).

61. Jacobs, T. A. Giedt, R. R., and Cohen, N., J. Chem. Phys. 43, 3688 (1965).

62. Blauer, J. A., J. Phys. Chem. 72, 79 (1968).

63. Fishburne, E. S., J. Chem. Phys. 45, 4053 (1966).

64. Jacobs, T. A. Cohen, N. and Giedt, R. R., J. Chem. Phys. 46, 1958 (1967).

65. Seery, D. J. and Bowman, C. T., J. Chem. Phys. $\underline{48}$, 4314 (1968).

66. Davies, W. O., "Radiative Energy Transfer on Entry into Mars and Venus," ITT Research Institute, Chicago, Illinois (Quarterly Report No. 8 to NASA) August 1964.

67. Presley, L. L., Chackerian, C., Jr., and Watson, R., "AIAA paper No. 66-518," 4th Aerospace Sciences Meeting, June 1966.

68. Fairbairn, A. R., Proc. Roy. Soc. A $\underline{312}$, 207 (1969).

69. Appleton, J. P., Steinberg, M., and Liquornik, D. J., Bull. Am. Phys. Soc. $\underline{13}$, 1603 (1968); also, J. Chem. Phys. $\underline{52}$, 2205 (1970).

70. Wray, K. L. and Teare, J. D., J. Chem. Phys. $\underline{36}$, 2582 (1962).

TABLE I. INTERACTION POTENTIAL PARAMETERS

(Morse Potential: V_{1M})

Species	From empirical rules			From curve-fitting	
	r_e (A)	U (^{o}K)	β (A^{-1})	r_e (A)	U (^{o}K)
H-Ar	2.91	130	1.44		
C-Ar	3.28	123	1.33		
N-Ar	3.18	200	1.49		380
O-Ar	3.10	220	1.44		
F-Ar	3.06	290	1.63		
Cℓ-Ar	3.39	384	1.41	2.4	900
Br-Ar	3.51	435	1.36	2.4	635
I-Ar	3.70	650	1.30	2.9	540

Table II. SPECTROSCOPIC DATA FOR THE MOLECULES

Species	Molecular State	Dissociation Products	Equilibrium Separation	Dissociation Energy	Electronic Degeneracy Factor	Vibrational Energy Spacing
			$r_e(\overset{\circ}{A})$	$U(_eV)$	$g_{XY}/g_X g_Y$	$\omega(cm^{-1})$
H_2	$X\ ^1\Sigma_g^+$	$^2S + {}^2S$	0.742	4.477	1/4	4161
N_2	$X\ ^1\Sigma_g^+$	$^4S + {}^4S$	1.10	9.76	1/16	2358
	$A\ ^3\Sigma_u^+$	$^4S + {}^4S$	1.29	3.59	3/16	1461
O_2	$X\ ^3\Sigma_g^-$	$^3P + {}^3P$	1.21	5.12	1/27	1556
	$a\ ^1\Delta_g$	$^3P + {}^3P$	1.22	4.14	2/81	1483
	$b\ ^1\Sigma_g^+$	$^3P + {}^3P$	1.23	3.49	1/81	1405
	$C\ ^3\Delta_u^+$	$^3P + {}^3P$	1.46	0.86	2/27	820
	$A\ ^3\Sigma_u^+$	$^3P + {}^3P$	1.42	0.78	1/27	775
	$c\ ^1\Sigma_u^-$	$^3P + {}^3P$	1.61	0.62	1/81	616
F_2	$X\ ^1\Sigma_g^+$	$^2P + {}^2P$	1.41	1.63	1/16	923
Cl_2	$X\ ^1\Sigma_g^+$	$^2P_{3/2} + {}^2P_{3/2}$	1.99	2.51	1/16	560
Br_2	$X\ ^1\Sigma_g^+$	$^2P_{3/2} + {}^2P_{3/2}$	2.28	1.97	1/16	323.2
	$A\ ^3\Pi_{1u}$	$^2P_{3/2} + {}^2P_{3/2}$	(2.9)	0.22	1/8	170.7
I_2	$X\ ^1\Sigma_g^+$	$^2P_{3/2} + {}^2P_{3/2}$	2.67	1.542	1/16	215
	$A\ ^3\Pi_{1u}$	$^2P_{3/2} + {}^2P_{3/2}$	(3.0)	0.07	1/8	44
HF	$X\ ^1\Sigma^+$	$^2S + {}^2P$	0.917	5.91	1/8	4139
HCl	$X\ ^1\Sigma^+$	$^2S + {}^2P$	1.275	4.43	1/8	2990

FIGURE CAPTIONS

Figure 1   Comparison between theoretical predictions of the recombination rate coefficient and experimental measurements for H_2, as a function of T. O, Larkin and Thrush,[26] and Larkin;[27] (H), Hurle et al.[28] (J), Jacobs et al;[29] (M;S), Myerson and Watt,[31] and Sutton.[30] Dashed curves: see text, Sec. 3.1.

Figure 2   Comparison between theoretical predictions of the recombination rate coefficient and experimental measure-ments for N_2, as a function of T. O, Clyne and Stedman;[33] ●, Campbell and Thrush;[32] (A), Appleton et al;[36] (B), Byron;[34] (C), Cary.[35] Full and dashed curves: see text, Sec. 3.2.

Figure 3   Comparison between theoretical predictions of the recombination rate coefficient and experimental measurements for O_2 as a function of T. ●, Campbell and Thrush;[37] O, Wray;[39] (W), Wray;[41] (WM), Watt and Myerson.[40] Dashed curves: see text, Sec. 3.3.

Figure 4   Comparison between theoretical predictions of the dissociation rate coefficient and experimental measurements for O_2, as a function of T. (W), Wray;[41] (CV), Camac and Vaughan;[42] (A), Anderson;[43] (WM), Watt and Myerson.[40] Dashed curves: see text, Sec. 3.3.

Figure 5   Comparison between theoretical predictions of the dissociation rate coefficient for F_2, and the experimental measurements taken from Johnson and Britton.[44] Dashed curve: see text, Sec. 3.4.

Table II. Cont.

CO	X $^1\Sigma^+$	$^3P + ^3P$	1.128	11.1	1/81	2170
	a $^3\Pi$	$^3P + ^3P$	1.206	5.09	2/27	1744
	a´ $^3\Sigma^+$	$^3P + ^3P$	1.352	4.24	1/27	1231
	d $^3\Delta$	$^3P + ^3P$	1.370	3.58	2/27	1153
	e $^3\Sigma^-$	$^3P + ^3P$	1.383	3.33	1/27	1114
	I $^1\Sigma^-$	$^3P + ^3P$	1.416	2.96	1/81	1064
	A $^1\Pi$	$^3P + ^3P$	1.235	3.08	2/81	1516
NO	X $^2\Pi$	$^4S + ^3P$	1.15	6.51	1/9	1876
	a $^4\Pi$	$^4S + ^3P$	1.39	1.80	2/9	995

Figure 6   Comparison between theoretical predictions of the re-
combination rate coefficient and experimental measurements for
Cl_2, as a function of T. ●, Clyne and Stedman;[45] (D), Diesen
and Felmlee;[46] (C), Van Thiel et al,[47] Carabetta and Palmer,[48]
and Jacobs and Giedt.[49] Full and dashed curves: see text, Sec.
3.4.

Figure 7   Comparison between theoretical predictions of the recombination
rate coefficient and experimental measurements for Br_2, as a
function of T. ●, Ip and Burns;[11,50] (A), Johnson and
Britton,[53] Warshay,[54] Britton,[55] and Palmer and Hornig,[56],
as summarized by Ip and Burns;[51] (E), emission measurements of
Boyd et al.[52] Full and dashed curves: see text, Sec. 3.4.

Figure 8   Comparison between theoretical predictions of the recombination
rate coefficient and experimental measurements for I_2, as a
function of T. O, Porter and Smith;[58] (BD), Bunker and
Davidson;[57] (BDGS), Britton et al;[59] (T), Troe and Wagner.[60]
Full and dashed curves: see text, Sec. 3.4.

Figure 9   Comparison between theoretical predictions of the dissociation
rate coefficient and experimental measurements for HF, as a
function of T. O, Jacobs et al;[61] (B), Blauer.[62] Long
dashed and short dashed curves: see text, Sec. 3.5.

Figure 10   Comparison between theoretical predictions of the dissociation
rate coefficient and experimental measurements for HCl, as a
function of T. Point measurements: Seery et al;[65] (F),
Fishburne;[63] (J), Jacobs et al.[64] Long dashed and short
dashed curves: see text, Sec. 3.5.

Figure 11   Comparison between theoretical predictions of the dissociation
            rate coefficient and experimental measurements for CO, as a
            function of T.   Point measurements: Appleton et al;[69] Shaded
            area: Davies,[66] and Presley.[67] Dashed curves: see text,
            Sec. 3.6.

Figure 12   Comparison between theoretical predictions of the recombination
            rate coefficient and experimental measurements for NO, as a
            function of T.   ●, Campbell and Thrush;[38] (W), Wray and Teare.[70]
            Dashed curves: see text, Sec. 3.6.

FIGURE 1

The axes of the figure are labeled: vertical axis "RECOMBINATION RATE COEFFICIENT, k_r cm^6 molecules^{-2} sec^{-1}" with gridline values 10^{-31}, 10^{-32}, 10^{-33}, 10^{-34}, 10^{-35}; horizontal axis "TEMPERATURE, T °K" with values 10^2, 10^3, 10^4. The plot is labeled N_2, with regions marked (B), (C), and (A).
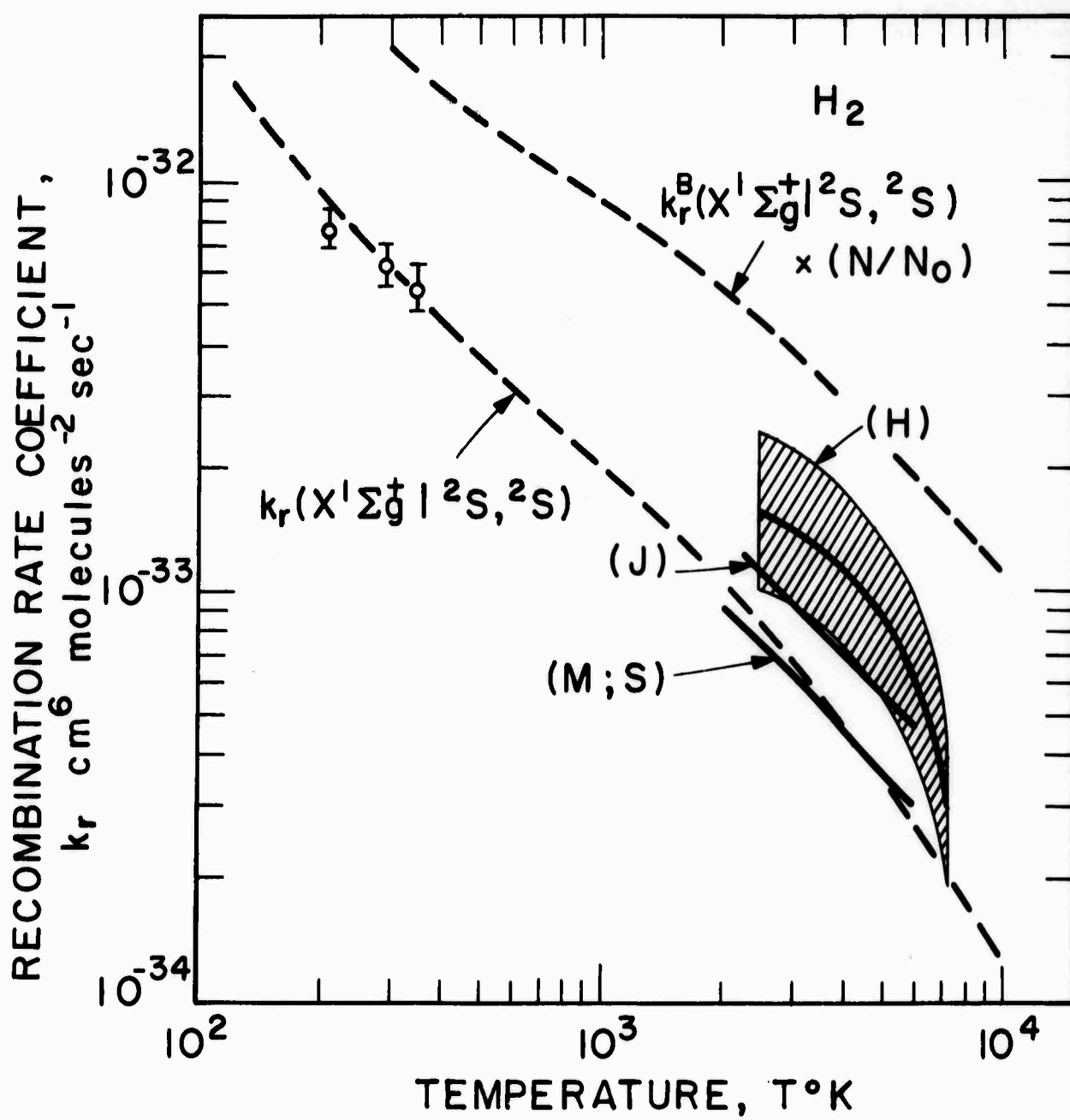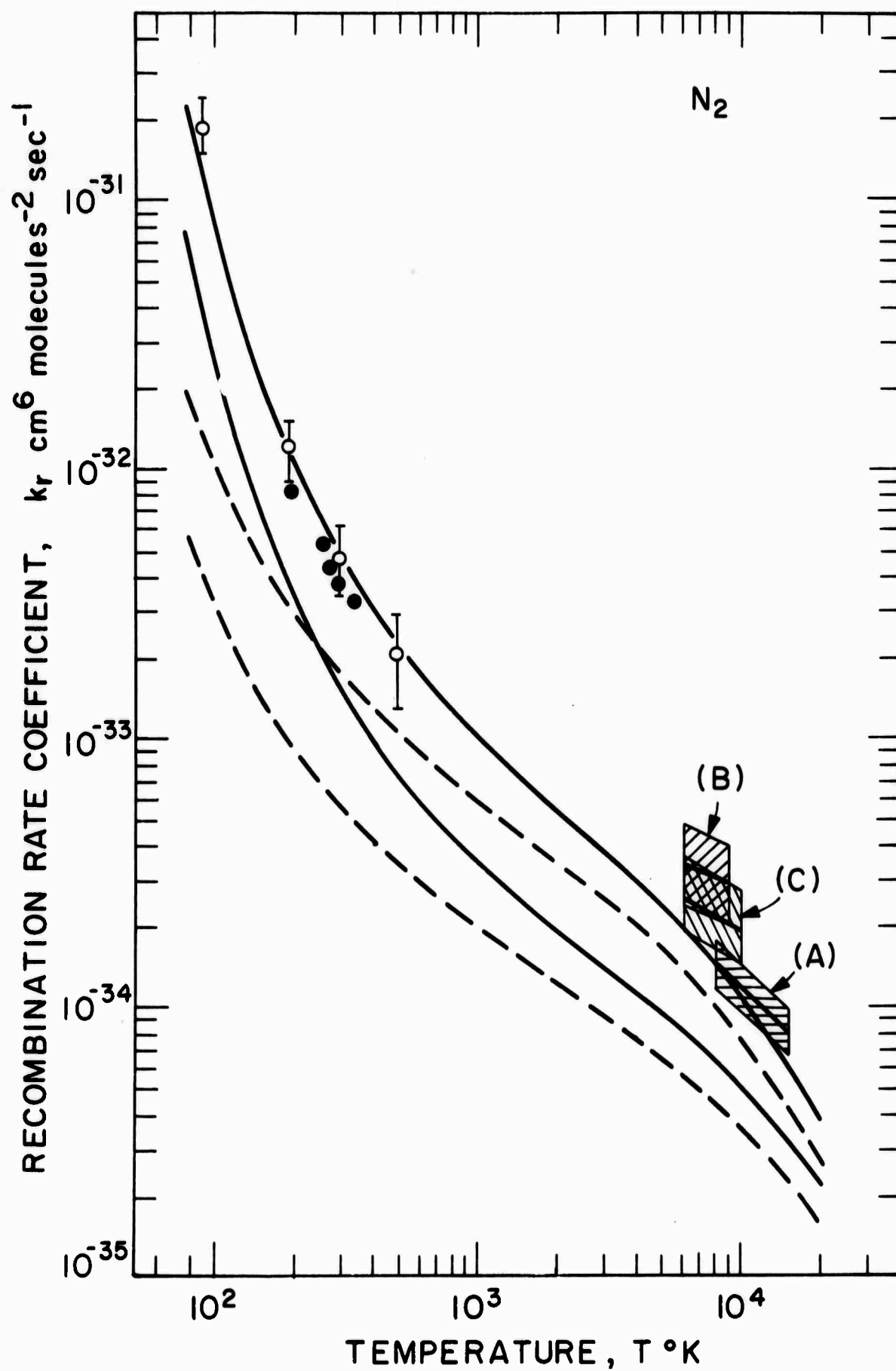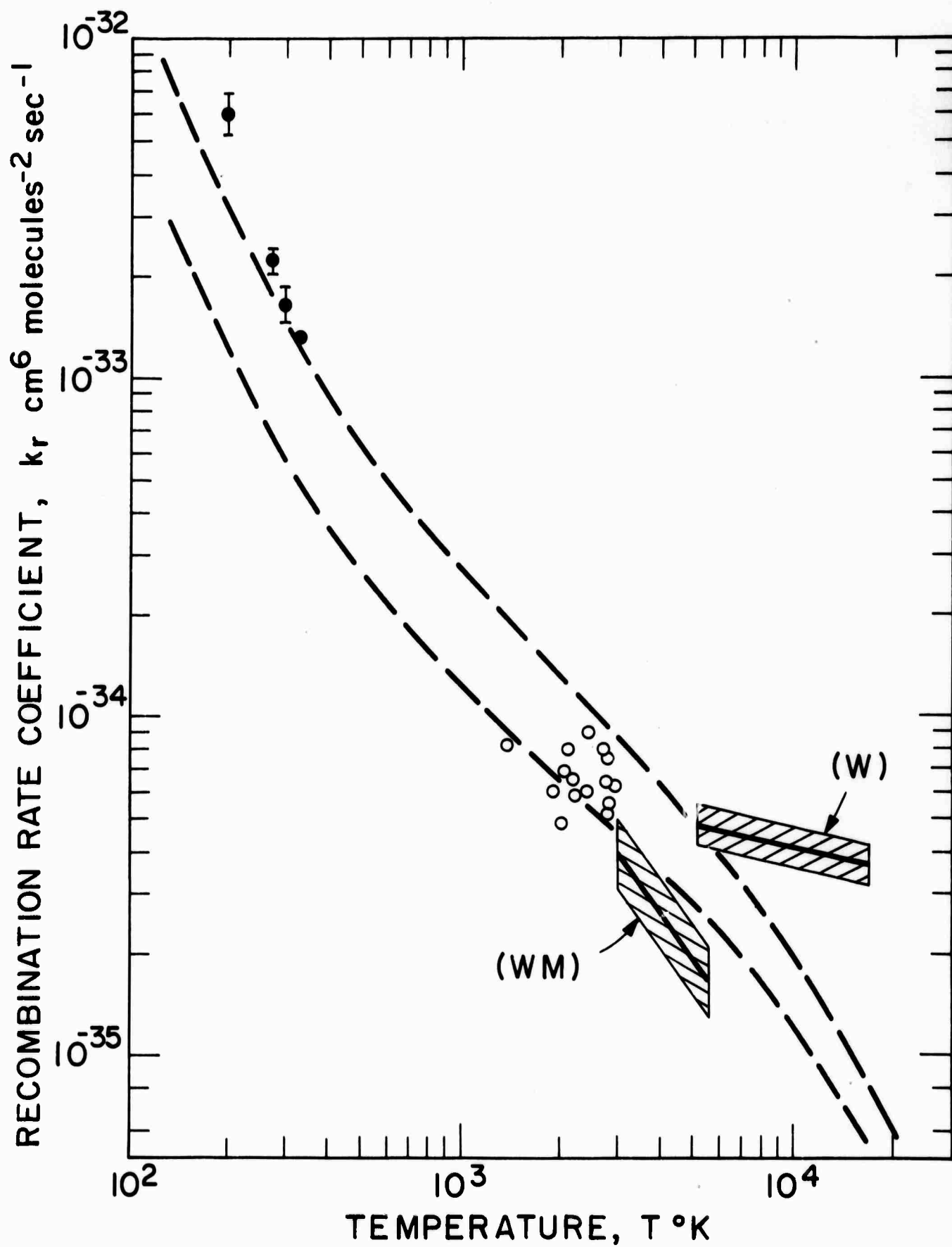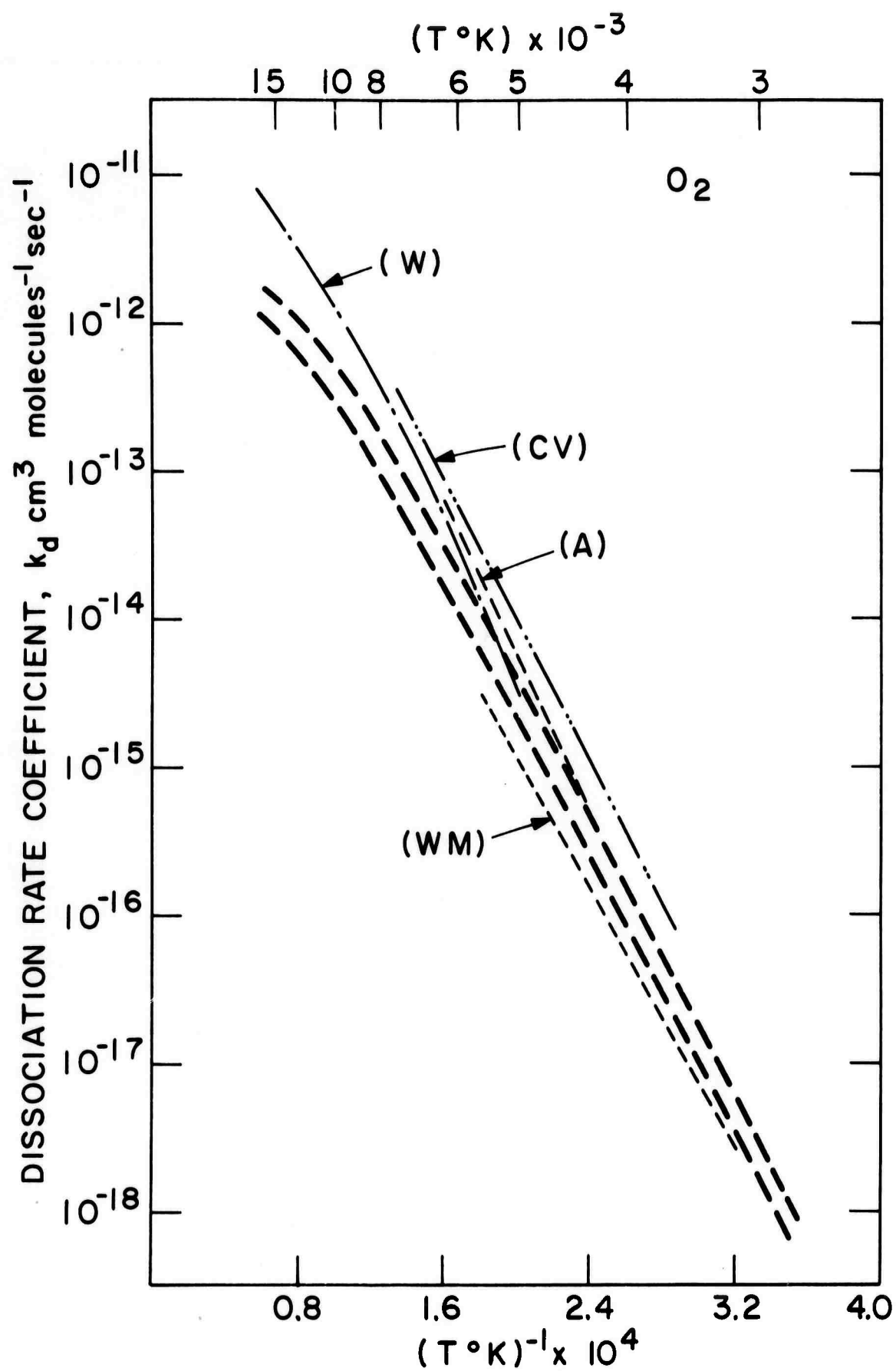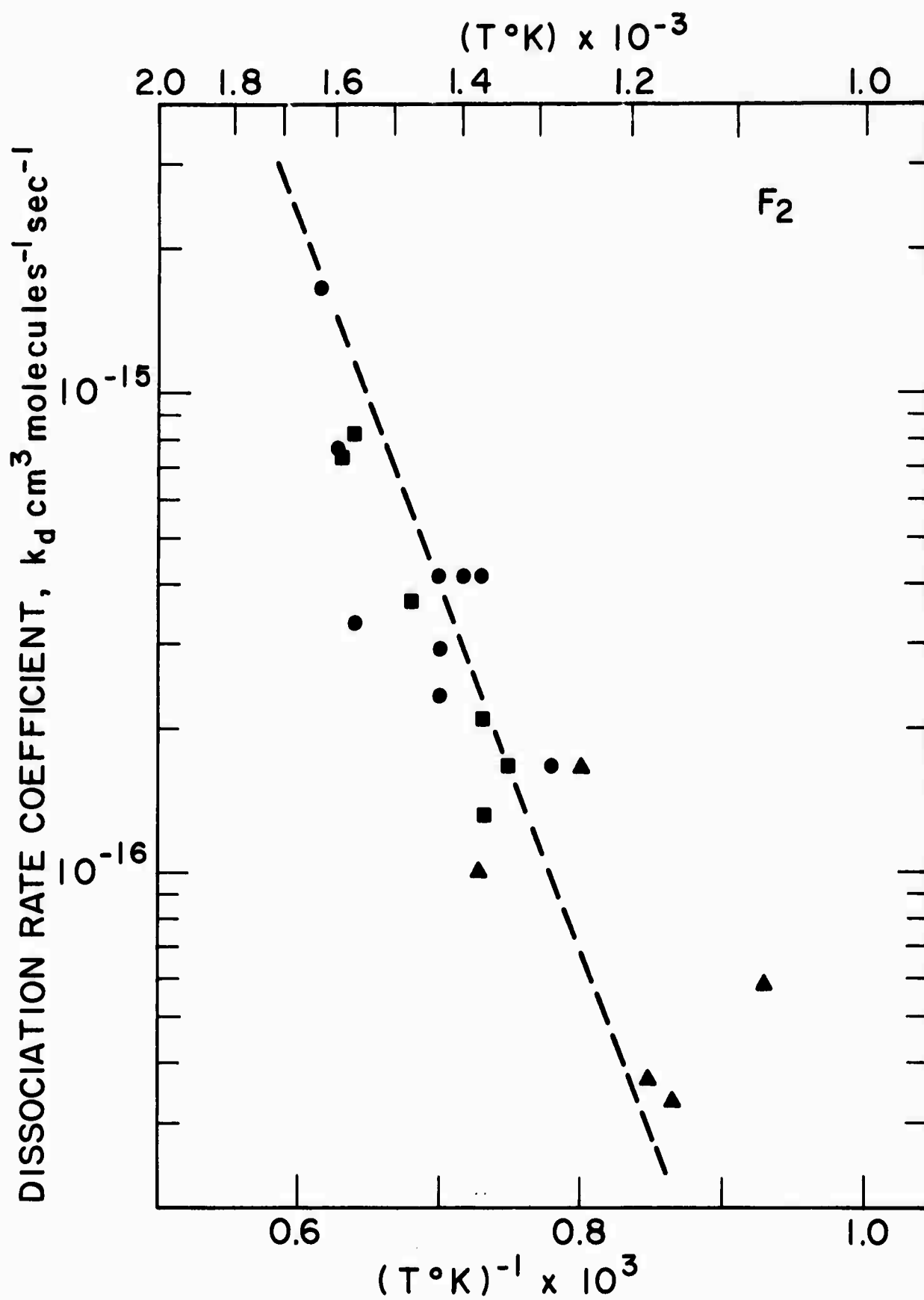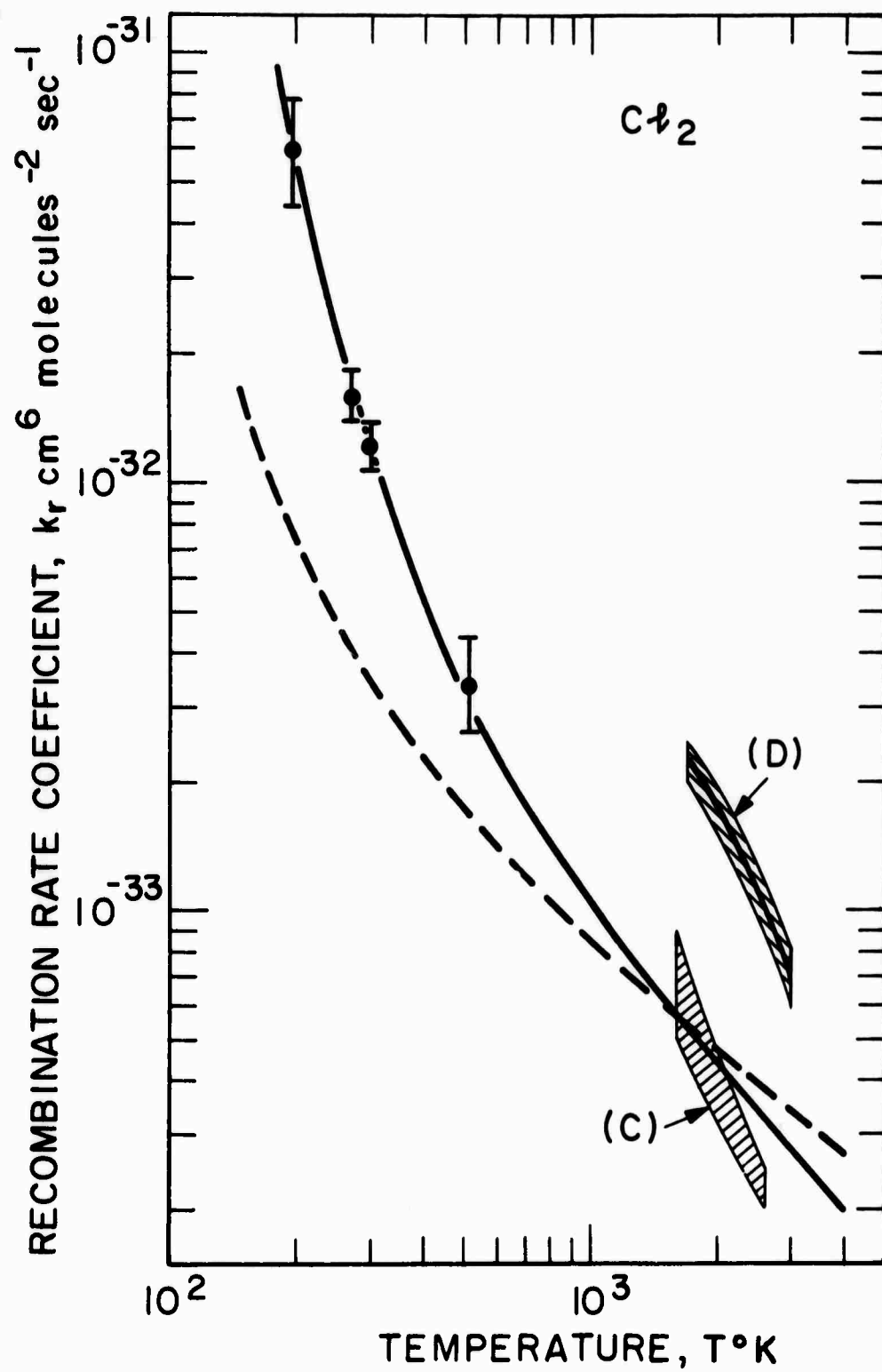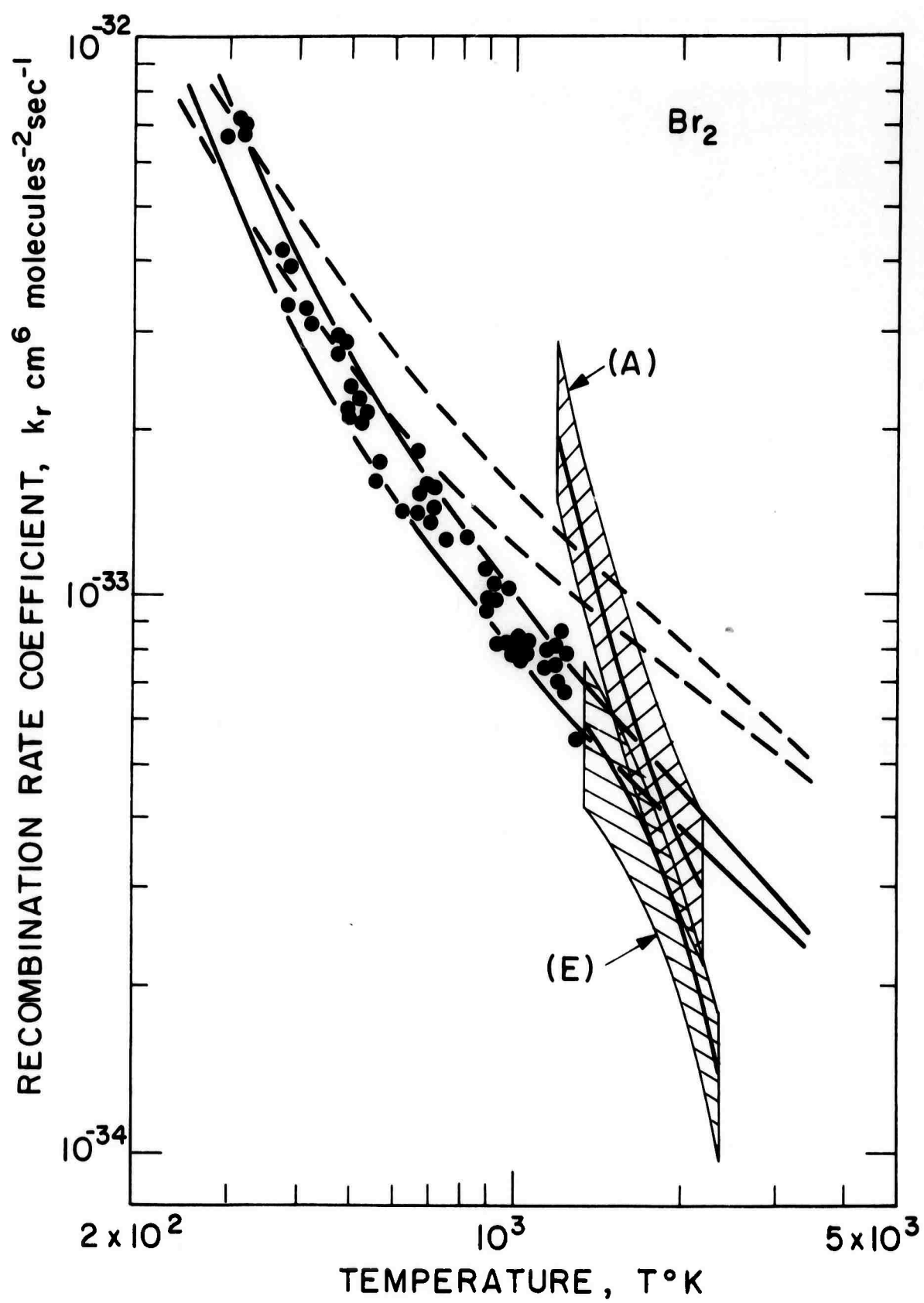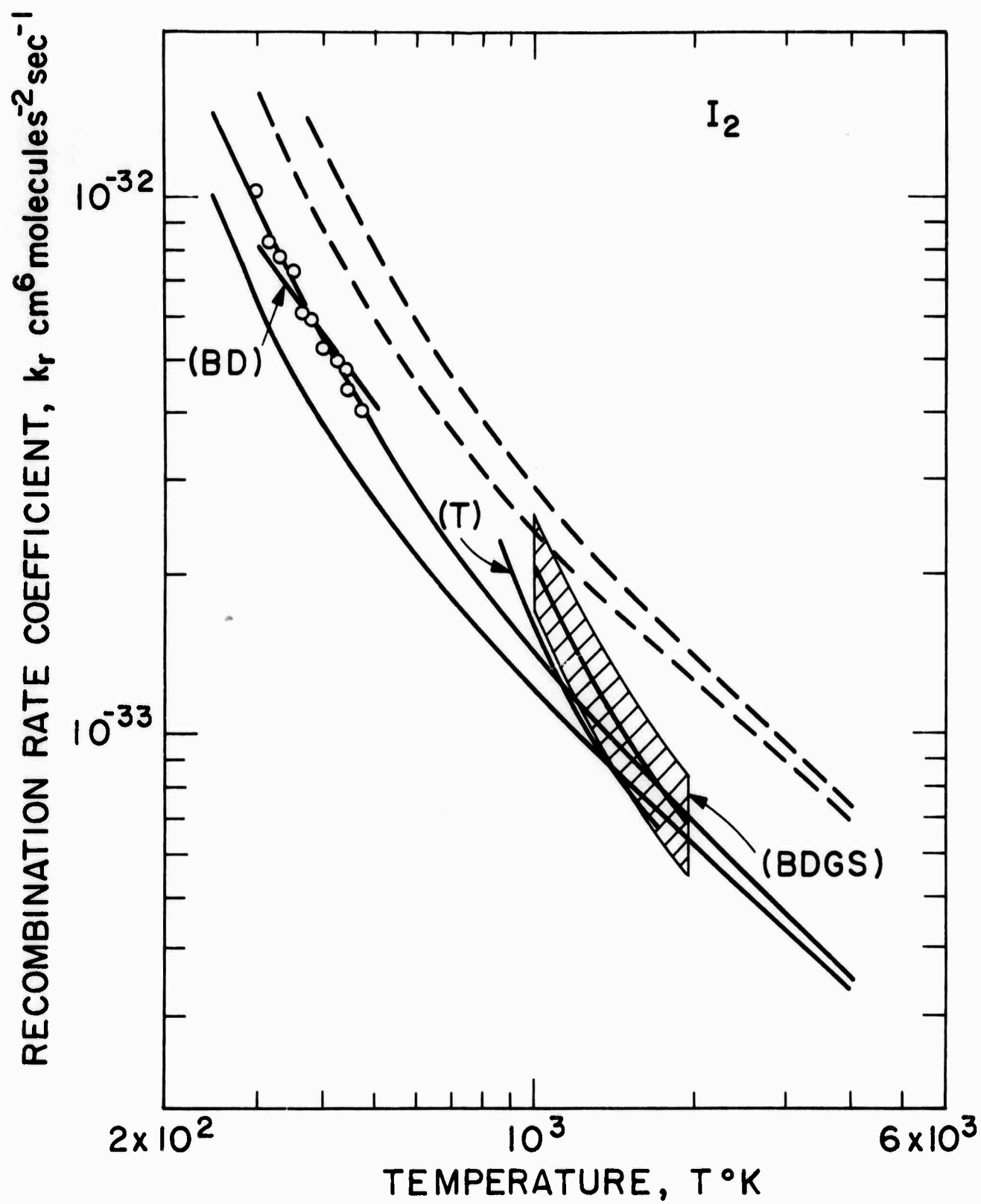
FIGURE 2

FIGURE 3

FIGURE 4

FIGURE 5

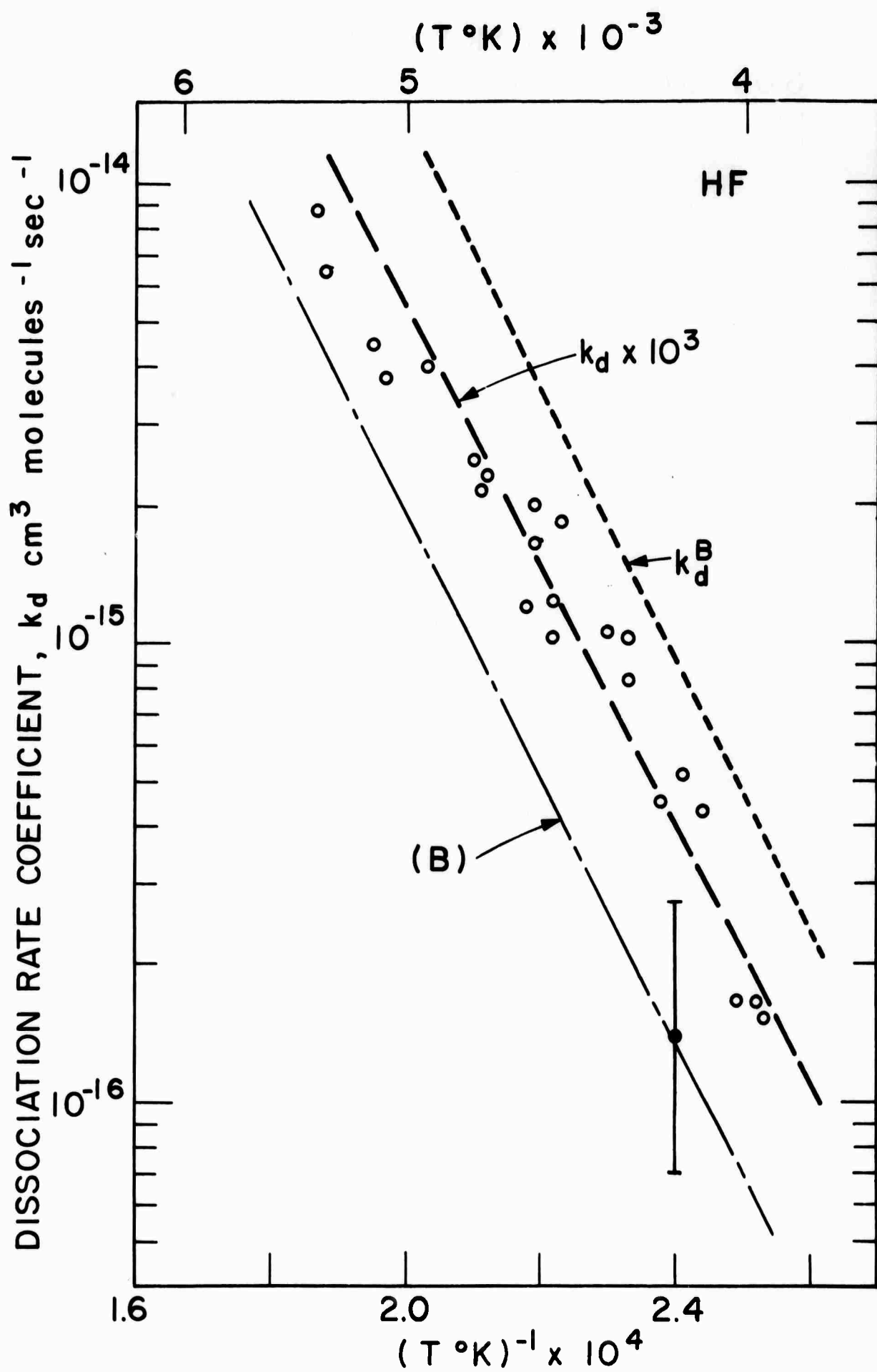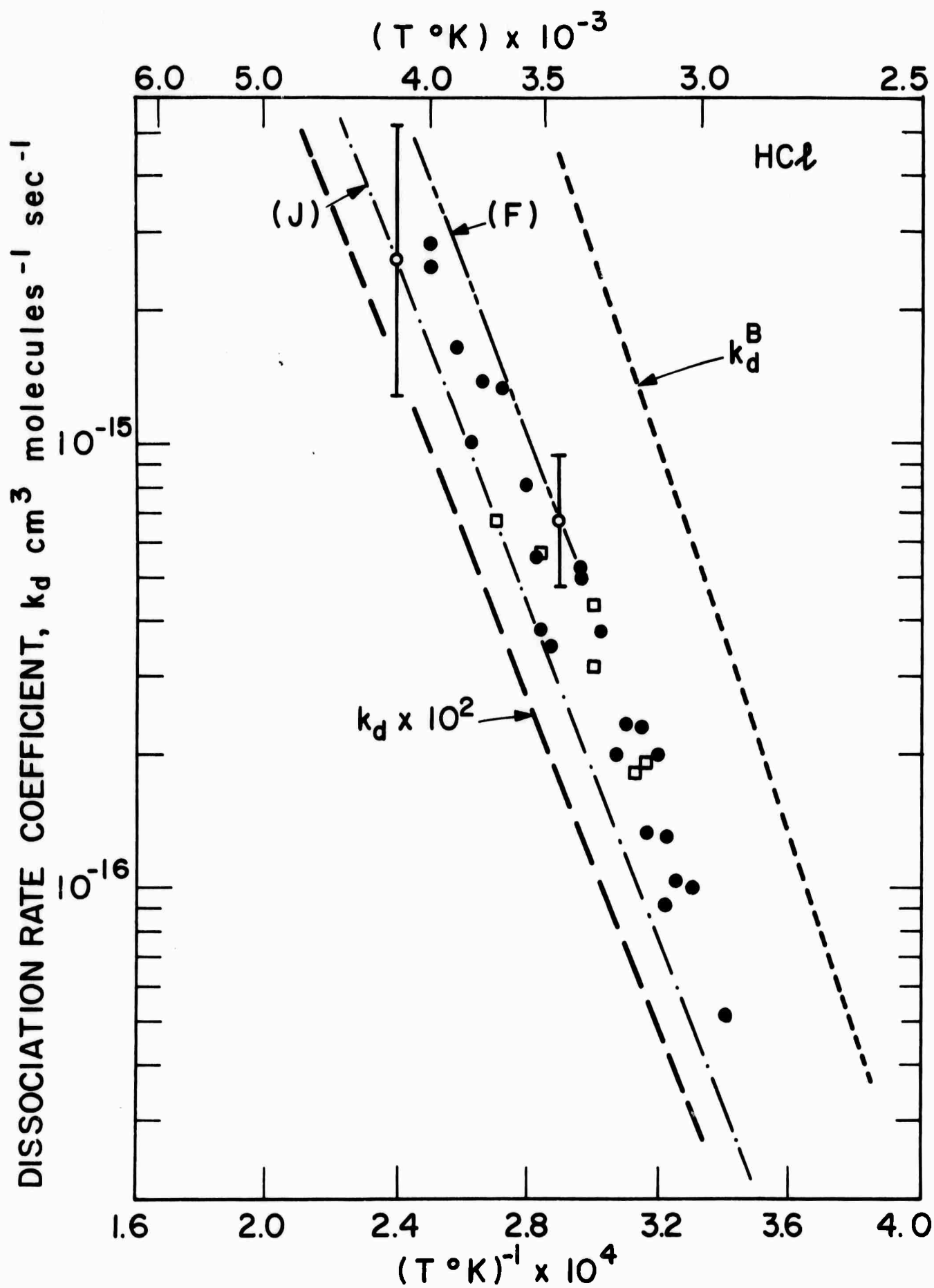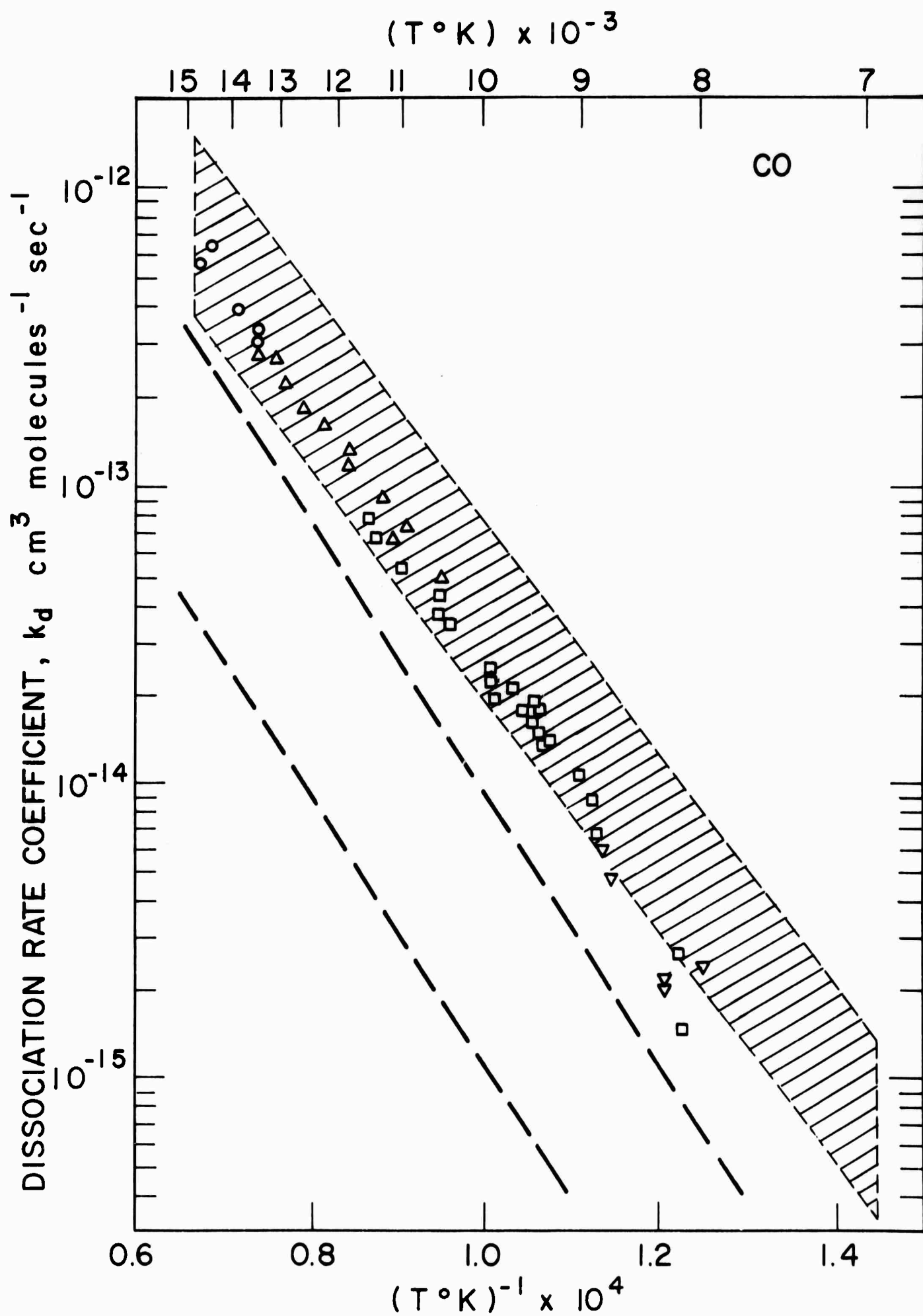FIGURE 6

FIGURE 7

FIGURE 8

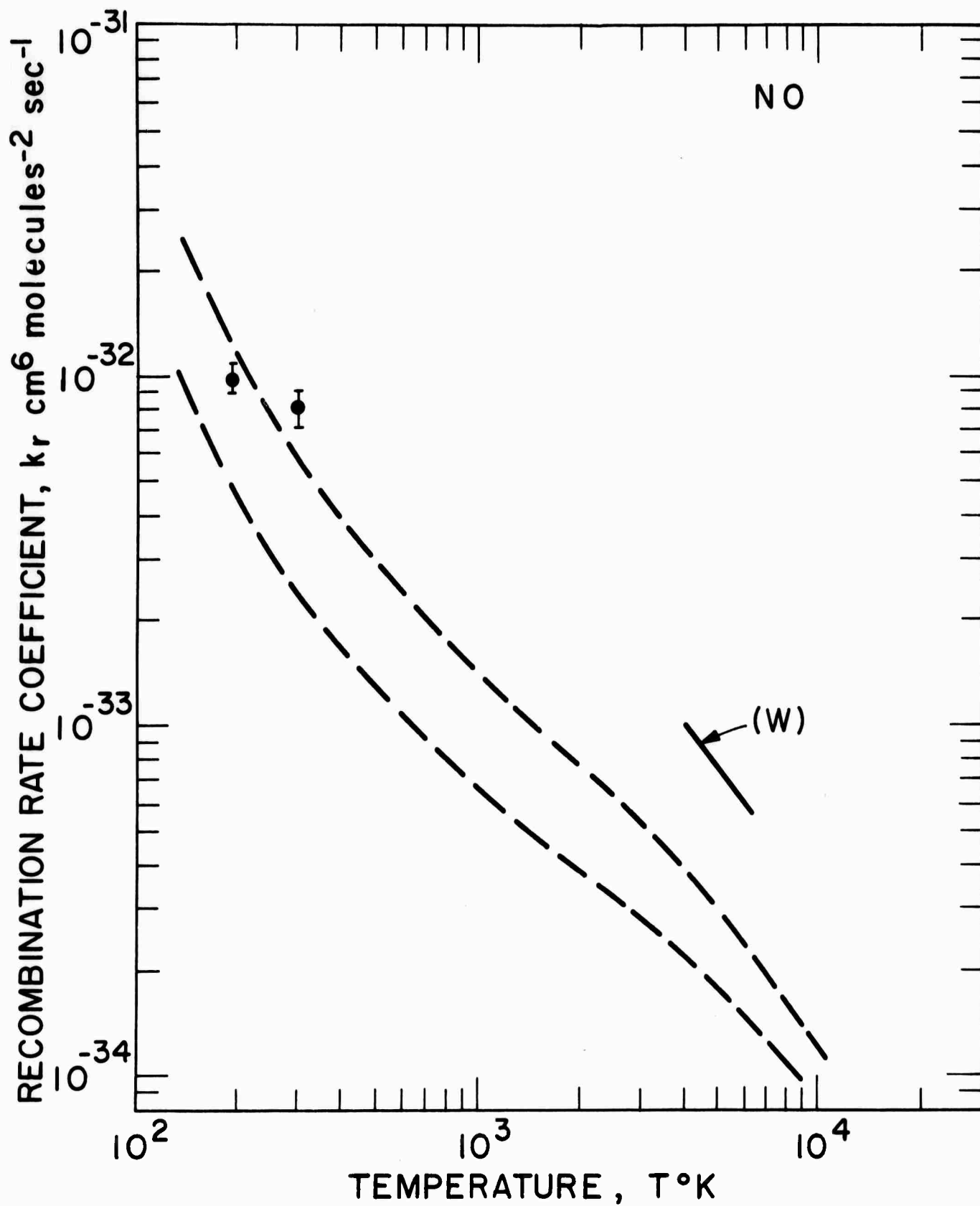FIGURE 9

FIGURE 10

FIGURE 11

FIGURE 12

DOCUMENT CONTROL DATA - R&D

(Security classification of title, body of abstract and indexing annotation must be entered when the overall report is classified)

1. ORIGINATING ACTIVITY (Corporate author)	2a. REPORT SECURITY CLASSIFICATION
M.I.T., Cambridge, Massachusetts	Unclassified
	2b. GROUP

3. REPORT TITLE

The Three-Body Recombination and Dissociation of Diatomic Molecules:
A Comparison Between Theory and Experiment

4. DESCRIPTIVE NOTES *(Type of report and inclusive dates)*

5. AUTHOR(S) *(Last name, first name, initial)*

Ven H. Shui, John P. Appleton and James C. Keck

6. REPORT DATE	7a. TOTAL NO. OF PAGES	7b. NO. OF REFS
April, 1970	26	70

8a. CONTRACT OR GRANT NO.	9a. ORIGINATOR'S REPORT NUMBER(S)
b. PROJECT NO. Office of Naval Research Contract No. N0014-67-A-0204-0040	Fluid Mechanics Laboratory Publication No. 70-3
c. and ARPA Order No. 322.	9b. OTHER REPORT NO(S) *(Any other numbers that may be assigned this report)*
d.	

10. AVAILABILITY/LIMITATION NOTICES

Distribution unlimited

11. SUPPLEMENTARY NOTES	12. SPONSORING MILITARY ACTIVITY
	Advanced Research Projects Agency of the Department of Defense and Office of Naval Research, Washington, D.C.

13. ABSTRACT

The modified phase-space theory of reaction rates has been used to predict the three-body recombination and dissociation rate coefficients of the diatomic gas molecules: H_2, N_2, O_2, F_2, Cl_2, Br_2, I_2 HF, HCl, CO, and NO, in the presence of argon as a collision partner. The ability of the theory to quantitatively predict and correlate both low temperature recombination rate measurements and high temperature dissociation rate measurements is substantial. The success of the theory clearly illustrates the importance of the weak attractive forces between the recombining atoms and argon atoms for recombination at low temperatures, the marked reduction in the rates at high temperatures due to nonequilibrium distributions in the vibrational state populations of the molecules, and the major contributions to reaction progress via electronically excited molecular states at all temperatures for such molecules as N_2 and CO.

DD FORM 1473   11A 0101 807 6800
1 JAN 64

14. KEY WORDS	LINK A		LINK B		LINK C	
	ROLE	WT	ROLE	WT	ROLE	WT
recombination						
dissociation						
phase-space theory						
hydrogen						
nitrogen						
oxygen fluorine						
chlorine						
bromine						
iodine						
hydrogen fluoride						
hydrogen chloride						
carbon monoxide						
nitric oxide						

INSTRUCTIONS

1. ORIGINATING ACTIVITY: Enter the name and address of the contractor, subcontractor, grantee, Department of Defense activity or other organization (*corporate author*) issuing the report.

2a. REPORT SECURITY CLASSIFICATION: Enter the overall security classification of the report. Indicate whether "Restricted Data" is included. Marking is to be in accordance with appropriate security regulations.

2b. GROUP: Automatic downgrading is specified in DoD Directive 5200.10 and Armed Forces Industrial Manual. Enter the group number. Also, when applicable, show that optional markings have been used for Group 3 and Group 4 as authorized.

3. REPORT TITLE: Enter the complete report title in all capital letters. Titles in all cases should be unclassified. If a meaningful title cannot be selected without classification, show title classification in all capitals in parenthesis immediately following the title.

4. DESCRIPTIVE NOTES: If appropriate, enter the type of report, e.g., interim, progress, summary, annual, or final. Give the inclusive dates when a specific reporting period is covered.

5. AUTHOR(S): Enter the name(s) of author(s) as shown on or in the report. Enter last name, first name, middle initial. If military, show rank and branch of service. The name of the principal author is an absolute minimum requirement.

6. REPORT DATE: Enter the date of the report as day, month, year; or month, year. If more than one date appears on the report, use date of publication.

7a. TOTAL NUMBER OF PAGES: The total page count should follow normal pagination procedures, i.e., enter the number of pages containing information.

7b. NUMBER OF REFERENCES: Enter the total number of references cited in the report.

8a. CONTRACT OR GRANT NUMBER: If appropriate, enter the applicable number of the contract or grant under which the report was written.

8b, 8c, & 8d. PROJECT NUMBER: Enter the appropriate military department identification, such as project number, subproject number, system numbers, task number, etc.

9a. ORIGINATOR'S REPORT NUMBER(S): Enter the official report number by which the document will be identified and controlled by the originating activity. This number must be unique to this report.

9b. OTHER REPORT NUMBER(S): If the report has been assigned any other report numbers (*either by the originator or by the sponsor*), also enter this number(s).

10. AVAILABILITY/LIMITATION NOTICES: Enter any limitations on further dissemination of the report, other than those

imposed by security classification, using standard statements such as:

   (1) "Qualified requesters may obtain copies of this report from DDC."

   (2) "Foreign announcement and dissemination of this report by DDC is not authorized."

   (3) "U. S. Government agencies may obtain copies of this report directly from DDC. Other qualified DDC users shall request through

                            ."

   (4) "U. S. military agencies may obtain copies of this report directly from DDC. Other qualified users shall request through

                            ."

   (5) "All distribution of this report is controlled. Qualified DDC users shall request through

                            ."

If the report has been furnished to the Office of Technical Services, Department of Commerce, for sale to the public, indicate this fact and enter the price, if known.

11. SUPPLEMENTARY NOTES: Use for additional explanatory notes.

12. SPONSORING MILITARY ACTIVITY: Enter the name of the departmental project office or laboratory sponsoring (*paying for*) the research and development. Include address.

13. ABSTRACT: Enter an abstract giving a brief and factual summary of the document indicative of the report, even though it may also appear elsewhere in the body of the technical report. If additional space is required, a continuation sheet shall be attached.

It is highly desirable that the abstract of classified reports be unclassified. Each paragraph of the abstract shall end with an indication of the military security classification of the information in the paragraph, represented as *(TS)*, *(S)*, *(C)*, or *(U)*.

There is no limitation on the length of the abstract. However, the suggested length is from 150 to 225 words.

14. KEY WORDS: Key words are technically meaningful terms or short phrases that characterize a report and may be used as index entries for cataloging the report. Key words must be selected so that no security classification is required. Identifiers, such as equipment model designation, trade name, military project code name, geographic location, may be used as key words but will be followed by an indication of technical context. The assignment of links, roles, and weights is optional.